Live cell single molecule tracking and localization microscopy of bioorthogonally labeled plasma membrane proteins

Andres I. König[1,2$], Raya Sorkin [3$], Ariel Alon[1,2], Dikla Nachmias[1,2], Kalyan Dhara [5], Guy Brand [3], Ofer Yifrach[1], Yael Roichman [3,4], Eyal Arbely [1,2,5], Natalie Elia[1,2]

[1] Department of Life Sciences, Ben-Gurion University of the Negev, Beer Sheva 84105, Israel

[2] National Institute for Biotechnology in the Negev (NIBN), Ben-Gurion University of the Negev, Beer Sheva 84105, Israel

[3] Raymond & Beverly Sackler School of Chemistry, Tel Aviv University, Tel Aviv 6997801, Israel

[4] Raymond & Beverly Sackler School of physics, and the Center for light-matter interaction, Tel Aviv University, Tel Aviv 6997801, Israel

[5] Department of Chemistry, Ben-Gurion University of the Negev, Beer Sheva 84105, Israel

$ Equal contribution

corresponding Author: Natalie Elia, Ph.D.

Email: elianat@post.bgu.ac.il

Fax: +972-8-6477546

Telephone: +972-8-6428735

Keywords: Kv channels, plasma membrane, quantitative imaging, receptors, super resolution microscopy, STORM, diffusion, protein clusters, click chemistry, fluorescent tags

ABSRACT

Tracking the localization and mobility of individual proteins in live cells is key for understanding how they mediate their function. Such information can be obtained from single molecule imaging techniques such as Single Particle Tracking (SPT) and Single Molecule Localization Microscopy (SMLM). Genetic code expansion (GCE) combined with bioorthogonal chemistry offers an elegant approach for direct labeling of proteins with fluorescent dyes, holding great potential for improving protein labeling in single molecule applications. Here we calibrated conditions for performing SPT and live-SMLM of bioorthogonally labeled plasma membrane proteins in live mammalian cells. Using SPT, the diffusion rates of bioorthogonally labeled EGF receptor and the prototypical Shaker voltage-activated potassium channel (Kv) were successfully measured. Applying live-SMLM to bioorthogonally labeled Shaker Kv channels enabled visualizing the plasma membrane distribution of the channel over time with ~30 nm accuracy. Finally, by competitive labeling with two Fl-dyes, SPT and live-SMLM were performed in a single cell and both the density and dynamics of the EGF receptor were measured at single molecule resolution in sub-regions of the cell. We conclude that GCE and bioorthogonal chemistry is a highly suitable, flexible approach for protein labeling in quantitative single molecule applications that outperforms current protein live cell labeling approaches.

Genetic code expansion (GCE) together with biorthogonal labeling offers an elegant tool for labeling proteins with organic Fluorescent dyes (Fl-dyes) in live mammalian cells. In GCE-based labeling, a non-canonical amino acid (ncAA) carrying a functional group is incorporated into the protein sequence in response to an in-frame amber stop codon (TAG), via an orthogonal tRNA/tRNA-synthetase pair (reviewed in [1,2]). Labeling is then carried out by a rapid and specific bioorthogonal reaction between the functional group and a Fl-dye. As a result, the protein of interest is fluorescently labeled on a specific residue, avoiding the need for conjugating protein tag fusions (i.e. fluorescent protein or self-labeling proteins) in live cell applications.

Direct labeling of proteins in live cells with Fl-dyes has several advantages for quantitative, high-end live cell imaging. First, Fl-dyes are bright and photostable and therefore cells can be imaged for longer times and at reduced laser intensities [3]. Second, the label itself is relatively small (Fl-dye, ~0.5 nm; GFP, 4.2 nm; antibodies >10nm; quantum dots 2-60 nm) thereby allowing higher accuracy in localization measurements and better representation of the physiological properties of the protein [3-5]. Third, labeling does not involve amplification, and therefore the number of molecules can be quantified. Fourth, the Fl-dye is applied at the last step of the reaction providing flexibility in optimizing the Fl-dye to specific applications and the possibility to simultaneously label the protein population with more than one dye [6]. Indeed, GCE and bioorthogonal labeling have been demonstrated, in recent years, in several microscopy techniques including live cell imaging and the super resolution microscopy techniques Structured Illumination Microscopy (SIM), Stimulated Emission Depletion (STED) and Single Molecule Localization Microscopy (SMLM) [6-11]. However, these studies focused

on the proof of concept and therefore very little quantitative information on the spatiotemporal dynamics of proteins in cells has been obtained from them.

Here we set out to perform quantitative analysis of the dynamics and spatial distribution plasma membrane (PM) proteins labeled via GCE and bioorthogonal chemistry. To this aim, we calibrated conditions for performing the live-cell single-molecule applications, Single Particle Tracking (SPT) and live-SMLM using extracellular bioorthogonal labeling. Using our optimized assay, significantly more tracks and longer trajectories were obtained for bioorthogonally labeled epidermal growth factor receptor (EGFR), compared to EGFR-GFP, increasing the reliability of the measurement and providing a more realistic representation of EGFR diffusion at the PM. Applying SPT to bioorthogonally-labeled prototypical Shaker B voltage dependent potassium channel, the diffusion rates of the channel in naïve and Latrunculin A (LatA) treated cells were measured, while data obtained from similar experiments using mCherry-Shaker B was not quantifiable. Together these results indicate that labeling proteins via GCE and bioorthogonal chemistry is superior to Fl-protein labeling for particle tracking. SMLM experiments of bioorthogonally labeled EGFR and Shaker B were successfully performed in fixed and live cells using our calibrated assay and allowed quantifying the dynamic distribution of PM proteins over time. Finally, using simultaneous labeling with two different Fl-dyes we performed live-SMLM and SPT in a single cell and determined the density and the dynamics of EGFR in subcellular regions at nanoscale resolution. Based on these results we conclude that bioorthogonal labeling of proteins is a suitable, improved and more flexible approach for quantitative live cell single molecule applications.

Calibrating conditions for SPT of bioorthogonally labeled PM proteins using EGFR

We began by testing the applicability of bioorthogonal labeling via GCE for single molecule imaging, EGFR, a well-studied receptor that has been previously labeled via GCE, was used as a benchmark [12]. To this end, EGFR was mutated to carry a TAG codon at the previously published labeling site, Leu 128, and cloned into a single expression vector that encodes the cognate pair of $tRNA_{cua}$:tRNA-synthetase [13,14] (Figure S1A). EGFR was then expressed in COS7 cells in the presence of the ncAA Bicyclo[6.1.0]nonyne-L-lysine (BCNK), which reacts bioorthogonally with tetrazine conjugated dyes (Figure 1A, left panel) [12,15]. Under these conditions specific plasma membrane labeling was obtained using the cell impermeable tetrazine conjugated Fl-dyes: AF647, Cy3, Cy5 or ATTO532, with Tet-Cy3 providing the most robust labeling, indicating that the $EGFR^{128BCNK}$ is efficiently expressed and targeted to the PM (Figure 1A).

Next, we tested the suitability of the different dyes for SPT, in vitro. This analysis was required because the tetrazine moiety is known to change the fluorogenicity of Fl-dyes and therefore may also affect their photophysical properties [2]. Among the Tet-conjugated dyes tested, Tet-Cy3 had the best overall properties for SPT applications; it was the brightest, produced the longest tracks and the largest number of tracks (Figure S1D). A uniform decoration of the PM was observed in cells expressing $EGFR^{128BCNK}$ labeled with Tet-Cy3 and imaged in TIRF mode, which indicates high labeling efficiencies but does not allow single molecules imaging. Under mild photobleaching conditions single molecules could be readily detected with relatively high signal to noise

ratio (SNR) (2.66 ± 0.45) (Figure 1 B). In cells expressing EGFR-GFP individual spots could be seen without photobleaching but were significantly dimer (SNR = 2.01 ± 0.27), indicating that bioorthogonal labeling provided higher labeling efficiencies and brighter spots (Figure 1 B, C and videos 1 and 2).

For tracking analysis, trajectories were extracted from videos of EGFR tagged with GFP (EGFR-GFP) or bioorthogonally labelled with Cy3 (EGFR-Cy3), recorded in TIRF mode at 20 msec intervals for up to three minutes (Figure 1 B, C). For each condition, videos recorded in at least three different independent experiments were used for the analysis. About 810 trajectories were obtained from each cell labeled via GCE (EGFR-Cy3) while only ~290 trajectories were obtained from cells expressing EGFR-GFP. This difference may result from the tendency of Fl-dyes to nonspecifically bind to membranes and to the glass bottom of the imaging chamber [3,16]. To avoid including these nonspecific stationary Fl-dye molecules in our measurements, we tracked fluorophores located outside the cells and calculated their mean square displacements (MSDs) and diffusion rates (Figure S2). We then used these background trajectories to filter out trajectories with similar MSD values (Figure S2E). To avoid bias, this analysis and background filtering was also applied to EGFR-GFP tracks (Figure S2D, F). After filtering, about 230 trajectories were obtained from each cell with EGFR labeled via GCE (EGFR-Cy3) and only ~140 trajectories were obtained from cells expressing EGFR-GFP. Moreover, tracks were considerably longer for bioorthogonally labeled EGFR compared to EGFR-GFP, allowing measuring diffusion at larger timescales (Figure 1 D). Under these conditions, mean square displacements and median diffusion rates were calculated for EGFR-GFP (0.36 μm^2/sec with 80%

confidence interval of 0.17-0.74 μm^2/sec) and for GCE-labeled EGFR (0.28 μm^2/sec with 80% confidence interval of 0.1-0.63 μm^2/sec) (Figure 1B, C, E). Collectively, these data indicate that bioorthogonal labeling with Fl-dyes outperforms GFP tagging for particle tracking; the larger number of tracks and their increased length improved the accuracy of the measurements and providing a more realistic view of EGFR dynamics in cells.

Measuring PM diffusion of the prototypic Kv channel, Shaker B, using bioorthogonal labeling and SPT

Convinced by the suitability of GCE-based labeling for SPT, we set out to study the dynamics of the Shaker B Kv channel. Tagging the channel with fluorescent proteins is challenging because its N and C termini are respectively engaged in the fast inactivation and clustering of the channel [17,18]. This is not a limitation in bioorthogonal labeling because the ncAA can be placed essentially anywhere in the protein. The Shaker Kv is a homotetrameric protein that open and closes in response to changes in membrane potential. Each subunit is comprised of six transmembrane helices, with helices 1-4 (S1-S4) constructing the voltage-sensing domain, and helices 5 and 6 making the selective pore domain (Figure 2A). We began by testing the suitability of several extracellular positions in Shaker B for bioorthogonal labeling: two positions in the loop linking helices S1-S2, K253 and I275, and one in the S3-S4 loop, V345. While almost no labeling was obtained in cells expressing Shaker $B^{K253BCNK}$ and Shaker $B^{I275BCNK}$, robust and specific PM labeling was obtained by encoding BCNK at position 345 in Shaker B (Figure 2A and Figure S3).

Interestingly, successful labeling of Shaker $B^{V345BCNK}$ was only obtained using Tet-Cy3 or Tet-Cy5, while no labeling was obtained using Tet-ATTO-532 or Tet-AF647 (Figure 2A). The S3-S4 loop in Shaker B resides in very close proximity to the plasma membrane, which may affect the binding or change the fluorescent properties of some Fl-dyes [19,20]. In order to overcome this effect, we inserted after position 344, a 14-residue long peptide linker that encodes for BCNK, which we have recently optimized (unpublished results, Figure S1C). Using this linker, specific PM labeling of Shaker B was obtained using any of the dyes tested, suggesting that displacing BCNK from the plasma membrane may improve labeling (Figure 2B and S1C). We therefore used the linker-based version of BCNK-Shaker B (Shaker $B^{linkerBCNK}$) in all future experiments.

SPT experiments were successfully performed for Shaker B, bioorthogonally labeled with Tet-Cy3. Approximately 160 tracks were obtained from each cell, after background filtering, with a median track length of 23 frames (compared to 126 tracks and median track length of 23 frames obtained for EGFR-Cy3), indicating that measurements are reliable. No trajectories could be generated upon applying similar experimental conditions to cells expressing mCherry-Shaker B due to a low signal to noise ratio (Figure S4A). This indicates that in addition to the potential artifacts associated with tagging the channel at the N terminal, the resulting signal is too dim for allowing particle tracking. The median diffusion rates obtained for Shaker B-Cy3 after thresholding was 0.21 μm^2/sec (with 80% confidence interval of 0.07-0.52 μm^2/sec) (Figure 2C and S4B, C). This value is 0.06 μm^2/sec slower than the diffusion rate obtained for EGFR-Cy3, indicating that the channel is 21% less mobile than the receptor. Applying the actin polymerization inhibitor, LatA to cells with bioorthogonally

labeled Shaker B, significantly increased the diffusion rate of the channel, essentially abolishing the difference between EGFR and Shaker B (Figure 2D). This indicates that, consistent with previous results, the actin cytoskeleton plays a role in controlling the dynamics of the Shaker B channel on the plasma membrane [21,22].

Performing live-SMLM on bioorthogonally labeled PM proteins

SMLM can be used to resolve the spatial distribution of PM proteins at ~30 nm resolution [23-25]. Bioorthogonal labeling is expected to be advantageous to SMLM; the small size of label improves the theoretical resolution of the technique and the superb photophysical properties of Fl-dyes enables acquisitions at reduced laser powers that may enable performing SMLM in live cell [3,16]. High density labeling is required in SMLM and especially in live-SMLM experiments for obtaining a “true” representation of protein distributions. Encouraged by the high labeling densities we obtained for EGFR and Shaker B in SPT experiments, we set to optimize conditions for live-SMLM of bioorthogonally labeled PM proteins. SMLM experiments were successfully performed in fixed COS7 cells expressing either $EGFR^{128BCNK}$ or $ShakerB^{linkerBCNK}$ and labeled with Tet-AF647 (Figure S5). More than 3,170 $\pm$ 553 localizations/μm^2 and 1,600 $\pm$ 583 localizations/μm^2 were obtained for EGFR and the Shaker Kv channel respectively, with an average localization uncertainty of 28.5 ±10.2 nm for EGFR and 23.3 ±6.9 nm for Shaker B.

Next, we calibrated conditions for live SMLM. First, we looked for SMLM buffers that induce efficient blinking of Tet-AF647 and are compatible with live cell imaging. We found OptiMEM supplemented with 5% glucose, a GLOXY oxygen scavenging system and 1% β-mercaptoethanol, suitable for extracellular live-SMLM. Second, we calibrated

the acquisition protocol. In classical SMLM experiments the number of new molecules that appear in each frame decreases overtime until the entire population of molecules is exhausted. However, for quantitative live imaging the number of localizations should be as similar as possible in each time point, in order to acquire representative data over time. The acquisition protocol was therefore adapted according to these needs (Figure S6). Last, we estimated temporal resolution. An SMLM image is built from a series of images hence, the temporal resolution should be set by the minimal number of frames needed for obtaining a representative image of the distribution of molecules across the PM. Based on SMLM experiments performed on bioorthogonaly-labeled Shaker Kv channels in fixed cells, we estimated that about 150 frames are needed for getting a representative SMLM image, providing a temporal resolution of 2.7 seconds (at 18 ms frame rate) (Figure S7).

Using these optimized conditions, live-SMLM experiments were successfully recorded in COS7 cells expressing GCE modified Shaker channels and labeled with Tet-AF647 (Figure 3). Live SMLM videos of Shaker B-AF647 were recorded for 27 seconds and each 150 frames were merged into a single timepoint. Approximately 28,000±4,500 localizations with an average uncertainty of 25.5±6.8 nm, were obtained in each timepoint. The entire time series was then overlaid using a color-coded map or played as a video (Figures 3 A-C and video 3). Substantial changes were observed at this temporal resolution for Fl-dye molecules positioned within the cell contour. Yet, almost no movements were recorded for Fl-dye molecules outside the cells, indicating that these changes do not result from drift (Figure 3C, blue arrow, steady particle; red arrows moving particles). At this temporal resolution, individual shaker B channels could

not be tracked overtime. However, a large-scale overview on the dynamic distribution of Shaker B channels at the PM over time was obtained. To quantitatively estimate these large-scale changes, we plotted the distribution of molecule densities over time. This analysis showed that the probability of a Shaker B channel to reside at low densities is high and does not change overtime, indicating that the overall distribution of Shaker B at the PM is relatively steady (Figure 3D). However, the probability of Shaker B to reside at high densities changed between different time points. Importantly, these changes were irregular and fluctuated differently in different cells, indicating that they do not result from the acquisition itself but rather reflect a change in the probability of Shaker B to arrange at high-density units (Figure 3D and S8). Shaker B is known to assemble into clusters at the PM [26,27]. Assuming that these high-density regions represent clusters of ShakerB, this data suggests that Shaker B clusters are dynamic and that they form, collapse or change their size within seconds or less.

Sequential live-SMLM and SPT acquisitions in single cells via simultaneous bioorthogonal labeling of EFGR with two dyes

In GCE-based bioorthogonal labeling of proteins, more than one Fl-dye can be applied at the labeling step, resulting in competitive labeling of the protein with different Fl-dyes [6]. This can potentially be used for performing SPT and live-SMLM, which requires Fl-dyes with different fluorescent properties, in the same cell. To this end, we expressed $EGFR^{128BCNK}$ in COS7 cells and applied both Tet-Cy3 and Tet-AF647 at the labeling step. Cells were imaged live in SMLM mode, using AF647 channel, and then in SPT mode, using Cy3 channel. Using this protocol, both the overall distribution of molecules overtime (live-SMLM) and the dynamics of single molecules at the PM (SPT)

were obtained from the same cell (Figure 4 A-D). Notably, such analysis allows correlating molecular densities and other spatial related information with diffusion rates at sub-regions of the cell, as demonstrated in (Figure 4 E).

To conclude, we showed that GCE-based biorthogonal labeling of proteins with Fl-dye could be used for live cell single molecule applications. Single particle tracking of EGFR that carries a ncAA at position 128 and labeled with Tet-cy3, outperformed particle tracking using EGFR tagged with GFP, and enabled measuring the diffusion of the potassium channel, Shaker B on the PM. Moreover, live-SMLM were successfully performed and allowed recording the distribution of Shaker B at the PM over time with ~30 nm accuracy. Finally, by combining these two approaches in a single cell, the distribution of EGFR at the PM was documented at nanoscale resolution (live-SMLM) and its diffusion rates were measured with high accuracy (SPT). This opens up the opportunity to relate protein diffusion with overall distribution, information that can shed light on the spatiotemporal changes plasma membrane proteins undergo upon activation / inactivation conditions, in subregions of the cell.

The SPT analysis of EGFR and the Shaker Kv channel resulted in higher diffusion rates compared to previously published values [22,28]. This can result from our stringent threshold criteria that were applied in order to ensure that background Fl-dye molecules that are not included in our measurements. We find this background thresholding crucial in this analysis due to the known stickiness of Fl-dyes. Given the robustness of our measurements, the increased track length and the minimal size of the label we believe that these values better reflect EFGR diffusion in cells. The diffusion rates obtained for EGFR were significantly higher than those measured for the Shaker

channel. This difference may result from the oligomeric state of the proteins (EGFR, dimer; Shaker B, tetramer) or from the binding of the Shaker channel to scaffold proteins such as PSD95 [26]. Consistent with previous reports, diffusion of the Shaker Kv channel, measured using SPT, was significantly higher upon Latranculin treatment, therefore validating our single particle tracking acquisition and analysis parameters [21,22].

High density labeling is key for the success of super resolution microscopy techniques and specifically for SMLM. To apply these methodologies using GCE and bioorthogonal based labeling we performed a series of calibration and optimization steps. Under our optimized conditions efficient labeling of EGFR and Shaker B at the plasma membrane were obtained with higher labeling efficiencies obtained for EGFR, which allowed performing localization microscopy of these proteins in fixed and live cells. In these experiments, we obtained a temporal resolution of ~ 2.5 sec (Figure 3). This temporal resolution was obtained using the maximum frame rate of the EMCCD-camera (55 fps) and may be further improved by using higher frame rate cameras. Moreover, the high labeling efficiencies obtained for $EGFR^{128BCNK}$ enabled SPT and live-SMLM to be recorded in the same cell. Because our microscope setup includes one camera, these datasets were recorded sequentially. Using a dual camera setup these datasets may be recorded in parallel, providing the opportunity to document both the distribution and the dynamics of PM proteins in real time.

MATERIALS AND METHODS

Cell culture

COS7 cells were grown in Dulbecco's Modified Eagle Medium supplemented with 10% fetal bovine serum (FBS), 2 mM glutamine, 10,000 U/ml penicillin, and 10 mg/ml streptomycin.

Genetic code expansion and bioorthogonal labeling in mammalian cells

For live cell experiments, cells were plated twenty-four hours before transfection with 15% confluency in four-well µ-Dish glass-bottom chamber slide (Ibidi, Martinsried, Germany). Transfection with the plasmids described in Figure S1 A-C, was carried out using Lipofectamine 2000 (Life Technologies, Carlsbad, CA) according to the manufacturer's guidelines. Genetic code expansion and biorthogonal labeling was carried out as described in Schvartz et al. [11]. In short, cells were incubated for 48 h in the presence of BCNK (0.5 mM; Synaffix, Oss, Netherlands) and washed with fresh medium at 37°C. Labeling was then carried out in the dark (30 min 37°C) with 1.5 µM of: Tet-Cy3, Tet-Cy5, Tet-ATTO532 (Jena Bioscience GmbH, Jena, Germany) or AF647 (Thermo Fisher Scientific, Waltham, MA), that was coupled with the tetrazine as previously described [9]. Finally, cells were washed again and imaged as described below. For performing SMLM-SPT in the same cell (Figure 4A), cells were incubated with both Tet-Cy3 (150 nm) and Tet-AF647 (1.5 µM).

Live cell imaging

Single Z-slices of selected labeled cells were collected at 37°C using a fully incubated confocal spinning-disk microscope (Marianas; Intelligent Imaging, Denver, CO) with a

63X N.A 1.4 oil immersion objective and were recorded on an electron-multiplying charge coupled device camera (pixel size, 0.079 μm; Evolve; Photometrics, Tucson, AZ). Image processing and analysis were done using SlideBook version 6 (Intelligent Imaging).

Live cell single molecule imaging

Images were collected on a Zeiss Elyra inverted wide field fluorescent microscope using a Zeiss 100X N.A 1.46 TIRF oil immersion objective. Excitation was achieved using solid-state lasers (488nm for GFP or 561nm for Tet-Cy3 and mCherry). Images were recorded on an electron-multiplying charge coupled device camera (iXon DU897, Andor, Belfast, Northern Ireland). For each SPT experiment at least 500 images and up to 10,000 were recorded with a frame rate of 50 fps. For the Cy3 labeled samples (EGFR-Cy3, ShakerB-Cy3) a short (~10 sec) bleaching step with laser intensities of ~20% was applied prior to image acquisition in order to lower particle density to enable single particles detection.

Single particle tracking

Movies of cells, recorded on different days, were quantified for each condition. Single particles were detected and tracked using a custom MATLAB (MathWorks, Natick, Massachusetts) code. The ensemble average mean squared displacement of traced particles was defined as the average over all particles of the squared displacement of each particle at time τ from its position at $\tau = 0$:

$$MSD(\tau) = 1/N \sum_{i=1}^{N} \left(x_i(\tau) - x_i(0)\right)^2$$

where $x_i(\tau)$ is the position of particle i at time τ, and N is the total number of tracked particles.

Background filtering was performed by measuring diffusion of nonspecific Fl-dye molecules attached to the glass bottom and including and excluding tracks with similar diffusion rates, as described in Figure S2. To avoid bias due to difference in trajectory lengths, MSD values for filtering purposes were calculated only for the first 10 frames of each trajectory.

The distribution of the diffusion coefficients was calculated using the time averaged MSD of each trajectory:

$$MSD_i(\Delta\tau) = \frac{1}{T-\Delta\tau}\sum_{\mathrm{t}=0}^{T-\Delta\tau}\left(x_i(\mathrm{t}+\Delta\tau) - x_i(t)\right)^2$$

Where i indicates a particle index and T is the total number of frames the particle was tracked.

The diffusion coefficient for each particle is then derived from the slope of the $MSD_i(\Delta\tau)$ for $\Delta\tau \leq 0.1\ sec$, which is the linear domain of the MSD, according to $D_i = \frac{MSD_i(\Delta\tau)}{4\Delta\tau}$. We have obtained the slope by linear least square fit and considered only results that had less than 0.01 standard regression error. We note that the ensemble and time average MSDs do not coincide, which is typical for protein diffusion in the PM [29].

Single Molecule Localization Microscopy (SMLM)

Images were collected on a Zeiss Elyra inverted wide field fluorescence microscope using a Zeiss 100X N.A 1.46 TIRF oil immersion objective as described in live cell single molecule section. Fixed samples were imaged in the following buffer: 50 mM

TRIS, 10 mM NaCl to pH=8.0 supplemented with 10% glucose (%W/V), GLOXY oxygen scavenging system (170U/mL Glucose oxidase, 1,400U/mL Catalase) and 10mM mercaptoethylamine (MEA). Live samples were imaged in OptiMEM™ (Gibco™; Dublin; Ireland) supplemented with 2 mM glutamine, 5% glucose (%W/V), GLOXY oxygen scavenging system (170U/mL Glucose oxidase, 1,400U/mL Catalase) and 1% β-mercaptoethanol (%V/V) (BME). During acquisition, 405 nm irradiation was applied in increasing amounts. 10,000 images were collected in each experiment with a frame-rate of 55 fps using irradiation intensities of ~1-3 kW/cm^2.

SMLM image analysis

Single particles were localized, fitted and reconstructed using ThunderSTORM [30]. Fixed SMLM localizations were filtered and drift corrected using cross-correlation before being reconstructed. In live SMLM, localizations were filtered, but drift corrected. Localizations obtained from 150 sequential frames were compiled into a single timepoint, using a custom written Python code (see optimization in Figure S7). Each frame was acquired at 18 msec. Density analysis (Figure 4D and S8) was performed for each time point using a custom written Python code, using a circular rolling window with a 50 nm radius. Number of particles were normalized for each time point. All codes are freely available at https://gitlab.com/sorkin.raya/storm-analysis.

Live SMLM-SPT imaging

COS7 cells were transfected as described above and bioorthogonally labeled with both Tet-Cy3 and Tet-AF647 (150 nM and 1.5 µM respectively). were first imaged in Live-SMLM as described above (5,000 frames) using a 640 nm channel. Then, Live-SMLM

buffer was substituted with growth media and the same cell was imaged for SPT. Videos were then processed for both live-SMLM and SPT as described above.

AUTHOR CONTRIBUTIONS

A.K and N.E designed and analyzed all experiments. A.K performed all experiments. A.A helped writing the manuscript. D.N and E.A provided technical help and knowledge in genetic code expansion. K.D and E.A synthesized Tet-AF647. R.S and Y.R did all SPT analysis and measurements. R.S and A.K generated the figures and sup figs. G.B and R.S performed density analysis in live-SMLM. O.Y contributed Shaker B plasmid and helped designing Shaker B mutants.

FUNDING SOURCES

The project leading to this application has received funding from European Research Council (ERC) under the European Union's Horizon 2020 research (N.E, startup grant). Y.R is supported by the ISF (Israel Science foundation) grant 988/17. R.S acknowledges support through HFSP postdoctoral fellowship LT000419/2015.

ACKNOWLEDGMENTS

We thank Ronit Pinkas-Kramarski (TAU, Israel) for contributing the EGFR plasmid. We also thank members of the Elia laboratory for fruitful discussions and for critical reading of the manuscript.

REFERENCES

1 Chin, J. W. Expanding and reprogramming the genetic code. *Nature* **550**, 53-60, doi:10.1038/nature24031 (2017).

2 Lang, K. & Chin, J. W. Cellular incorporation of unnatural amino acids and bioorthogonal labeling of proteins. *Chemical reviews* **114**, 4764-4806, doi:10.1021/cr400355w (2014).

3 van de Linde, S., Heilemann, M. & Sauer, M. Live-cell super-resolution imaging with synthetic fluorophores. *Annual review of physical chemistry* **63**, 519-540, doi:10.1146/annurev-physchem-032811-112012 (2012).

4 Resch-Genger, U., Grabolle, M., Cavaliere-Jaricot, S., Nitschke, R. & Nann, T. Quantum dots versus organic dyes as fluorescent labels. *Nature methods* **5**, 763-775, doi:10.1038/nmeth.1248 (2008).

5 Dean, K. M. & Palmer, A. E. Advances in fluorescence labeling strategies for dynamic cellular imaging. *Nature chemical biology* **10**, 512-523, doi:10.1038/nchembio.1556 (2014).

6 Nikic, I. & Lemke, E. A. Genetic code expansion enabled site-specific dual-color protein labeling: superresolution microscopy and beyond. *Current opinion in chemical biology* **28**, 164-173, doi:10.1016/j.cbpa.2015.07.021 (2015).

7 Neubert, F., Beliu, G., Terpitz, U., Werner, C., Geis, C., Sauer, M. & Doose, S. Bioorthogonal Click Chemistry Enables Site-specific Fluorescence Labeling of Functional NMDA Receptors for Super-Resolution Imaging. *Angewandte Chemie* **57**, 16364-16369, doi:10.1002/anie.201808951 (2018).

8 Nikic, I., Plass, T., Schraidt, O., Szymanski, J., Briggs, J. A., Schultz, C. & Lemke, E. A. Minimal tags for rapid dual-color live-cell labeling and super-resolution microscopy. *Angewandte Chemie* **53**, 2245-2249, doi:10.1002/anie.201309847 (2014).

9 Uttamapinant, C., Howe, J. D., Lang, K., Beranek, V., Davis, L., Mahesh, M., Barry, N. P. & Chin, J. W. Genetic code expansion enables live-cell and super-resolution imaging of site-specifically labeled cellular proteins. *Journal of the American Chemical Society* **137**, 4602-4605, doi:10.1021/ja512838z (2015).

10 Vreja, I. C., Nikic, I., Gottfert, F., Bates, M., Krohnert, K., Outeiro, T. F., Hell, S. W., Lemke, E. A. & Rizzoli, S. O. Super-resolution Microscopy of Clickable Amino Acids Reveals the Effects of Fluorescent Protein Tagging on Protein Assemblies. *ACS nano* **9**, 11034-11041, doi:10.1021/acsnano.5b04434 (2015).

11 Schvartz, T., Aloush, N., Goliand, I., Segal, I., Nachmias, D., Arbely, E. & Elia, N. Direct fluorescent-dye labeling of alpha-tubulin in mammalian cells for live cell and superresolution imaging. *Molecular biology of the cell* **28**, 2747-2756, doi:10.1091/mbc.E17-03-0161 (2017).

12 Lang, K., Davis, L., Wallace, S., Mahesh, M., Cox, D. J., Blackman, M. L., Fox, J. M. & Chin, J. W. Genetic Encoding of bicyclononynes and trans-cyclooctenes for site-specific protein labeling in vitro and in live mammalian cells via rapid fluorogenic Diels-Alder reactions. *Journal of the American Chemical Society* **134**, 10317-10320, doi:10.1021/ja302832g (2012).

13 Aloush, N., Schvartz, T., Konig, A. I., Cohen, S., Brozgol, E., Tam, B., Nachmias, D., Ben-David, O., Garini, Y., Elia, N. & Arbely, E. Live Cell Imaging of Bioorthogonally Labelled Proteins Generated With a Single Pyrrolysine tRNA Gene. *Scientific reports* **8**, 14527, doi:10.1038/s41598-018-32824-1 (2018).

14 Cohen, S. & Arbely, E. Single-Plasmid-Based System for Efficient Noncanonical Amino Acid Mutagenesis in Cultured Mammalian Cells. *Chembiochem : a European journal of chemical biology* **17**, 1008-1011, doi:10.1002/cbic.201500681 (2016).

15 Blackman, M. L., Royzen, M. & Fox, J. M. Tetrazine ligation: fast bioconjugation based on inverse-electron-demand Diels-Alder reactivity. *Journal of the American Chemical Society* **130**, 13518-13519, doi:10.1021/ja8053805 (2008).
16 Klein, T., Loschberger, A., Proppert, S., Wolter, S., van de Linde, S. & Sauer, M. Live-cell dSTORM with SNAP-tag fusion proteins. *Nature methods* **8**, 7-9, doi:10.1038/nmeth0111-7b (2011).
17 Zandany, N., Lewin, L., Nirenberg, V., Orr, I. & Yifrach, O. Entropic clocks in the service of electrical signaling: 'Ball and chain' mechanisms for ion channel inactivation and clustering. *FEBS letters* **589**, 2441-2447, doi:10.1016/j.febslet.2015.06.010 (2015).
18 Uversky, V. N. The most important thing is the tail: multitudinous functionalities of intrinsically disordered protein termini. *FEBS letters* **587**, 1891-1901, doi:10.1016/j.febslet.2013.04.042 (2013).
19 Posson, D. J., Ge, P., Miller, C., Bezanilla, F. & Selvin, P. R. Small vertical movement of a K+ channel voltage sensor measured with luminescence energy transfer. *Nature* **436**, 848-851, doi:10.1038/nature03819 (2005).
20 Thompson, A. D., Bewersdorf, J., Toomre, D. & Schepartz, A. HIDE Probes: A New Toolkit for Visualizing Organelle Dynamics, Longer and at Super-Resolution. *Biochemistry* **56**, 5194-5201, doi:10.1021/acs.biochem.7b00545 (2017).
21 O'Connell, K. M., Loftus, R. & Tamkun, M. M. Localization-dependent activity of the Kv2.1 delayed-rectifier K+ channel. *Proceedings of the National Academy of Sciences of the United States of America* **107**, 12351-12356, doi:10.1073/pnas.1003028107 (2010).
22 Tamkun, M. M., O'Connell K, M. & Rolig, A. S. A cytoskeletal-based perimeter fence selectively corrals a sub-population of cell surface Kv2.1 channels. *Journal of cell science* **120**, 2413-2423, doi:10.1242/jcs.007351 (2007).
23 Patterson, G. H. Fluorescence microscopy below the diffraction limit. *Seminars in cell & developmental biology* **20**, 886-893, doi:10.1016/j.semcdb.2009.08.006 (2009).
24 Henriques, R., Griffiths, C., Hesper Rego, E. & Mhlanga, M. M. PALM and STORM: unlocking live-cell super-resolution. *Biopolymers* **95**, 322-331, doi:10.1002/bip.21586 (2011).
25 Sauer, M. & Heilemann, M. Single-Molecule Localization Microscopy in Eukaryotes. *Chemical reviews* **117**, 7478-7509, doi:10.1021/acs.chemrev.6b00667 (2017).
26 Kim, E., Niethammer, M., Rothschild, A., Jan, Y. N. & Sheng, M. Clustering of Shaker-type K+ channels by interaction with a family of membrane-associated guanylate kinases. *Nature* **378**, 85-88, doi:10.1038/378085a0 (1995).
27 Tiffany, A. M., Manganas, L. N., Kim, E., Hsueh, Y. P., Sheng, M. & Trimmer, J. S. PSD-95 and SAP97 exhibit distinct mechanisms for regulating K(+) channel surface expression and clustering. *The Journal of cell biology* **148**, 147-158, doi:10.1083/jcb.148.1.147 (2000).
28 Xiao, Z., Zhang, W., Yang, Y., Xu, L. & Fang, X. Single-molecule diffusion study of activated EGFR implicates its endocytic pathway. *Biochemical and biophysical research communications* **369**, 730-734, doi:10.1016/j.bbrc.2008.02.084 (2008).
29 Krapf, D. Mechanisms underlying anomalous diffusion in the plasma membrane. *Current topics in membranes* **75**, 167-207, doi:10.1016/bs.ctm.2015.03.002 (2015).
30 Ovesny, M., Krizek, P., Borkovec, J., Svindrych, Z. & Hagen, G. M. ThunderSTORM: a comprehensive ImageJ plug-in for PALM and STORM data analysis and super-resolution imaging. *Bioinformatics* **30**, 2389-2390, doi:10.1093/bioinformatics/btu202 (2014).

FIGURE LEGENDS

Figure 1. **Bioorthogonal labeling with Fl-dyes enables single particle tracking of EGFR (A)** Left panel: schematic representation of the labeling strategy. The exrtracellular domain of EGFR (yellow) was mutated to carry the ncAA BCNK (red) at position 128. Labeling was obtained via a bioorthogonal reaction between BCNK and a tetrazine conjugated Fl-dye (green star). Panels 2-5: Live COS7 cells expressing $EGFR^{128BCNK}$ together with GCE components (Figure S1A) were labeled with 1.5 μM of: Tet-AF647, Tet-Cy3, Tet-Cy5 or Tet-ATTO532 and imaged using a spinning disk confocal microscope. Shown are single slices taken from the center of the cell. Scale bar = 10 μm. **(B,C)** COS7 cells transfected with GCE system plasmid and $EGFR^{128BCNK}$ and labeled with Tet-Cy3 or with EGFR-GFP were imaged in TIRF mode at 50 fps. Single molecule tracks were then obtained as described in the materials and methods section. Left panel: representative images of the first frame (the complete video sequences are provided in Videos 1 and 2). Middle panels: tracks taken from representative cells. The diffusion coefficient [D] of all particles tracked is displayed in right panels. EGFR-Cy3 median, 0.36 μm^2/sec (with 80% confidence interval of 0.17-0.74 μm^2/sec, n=1,680). EGFR-GFP median, 0.28 μm^2/sec (with 80% confidence interval of 0.1-0.63μm^2/sec, n=1,629). **(D)** The tracking time probability density function of EGFR-GFP (green) or EGFR-Cy3 (red). **(E)** Mean square displacement curves of cells expressing either EGFR-GFP (green) or EGFR-Cy3 (red) as a function of time. Thick lines are the ensemble means for each labeling type with error bars representing SEM. Thin lines represent measurements obtained from individual cells (EGFR-Cy3 n=9 cells, EGFR-GFP n=17 cells, obtained from three independent experiments).

Figure 2. **Measuring the PM dynamics of bioorthogonally labeled Kv channels. (A, B)** COS7 cells transfected with the GCE system plasmid and ShakerB^{V345BCNK} (**A**) or with Shaker B in which BCNK is encoded via a short 14AA linker (**B**) (Figure S1B, C) were labeled with a tetrazine conjugated Fl-dye, as indicated and imaged in a confocal spinning disk microscope. Shown are single slices taken from the center of the cell. Schematic representations of the labeling strategies are shown on the left. Scale bar = 10µm. **(C, D)** Single particle tracking of Shaker B-Cy3 in naïve cells (**C**) and in cells treated with 1µM Latrunculin A (LatA) (**D**). Left panels, tracks obtained in representative COS7 cells. Each track is represented by a different color. Middle panels: the distribution of diffusion coefficients [D] of all particles tracked. Naïve cells median, 0.22 μm^2/sec (with 80% confidence interval of 0.07-0.52 μm^2/sec, n=2,181). LatA treated cells median, 0.28 μm^2/sec (with 80% confidence interval of 0.11-0.59 μm^2/sec, n=7,055). Right panels: Mean square displacement curves of cells expressing either Shaker B-Cy3 (blue), Shaker B-Cy3 + LatA (cyan) or EGFR-Cy3 (red) as a function of time. EGFR curves are shown for comparison. Thick lines are the ensemble means for each labeling type with error bars representing SEM. Thin lines represent measurements obtained from individual cells (Shaker B-Cy3 n=16 cells, Shaker B-Cy3 + LatA n=27, EGFR-Cy3 n=9 cells, obtained from three independent experiments).

Figure 3. **Bioorthogonal labeling enables super-resolution imaging of Shaker B in live cells. (A)** A live-SMLM time stack image of a representative COS7 cell transfected with GCE system plasmid and Shaker B carrying BCNK via a peptide linker (Figure

S1C), labeled with 1.5 μM Tet-AF647. Timepoints are encoded by different colors. Each timepoint was reconstructed from 150 frames. A zoomed in image of the region depicted in black square in top panel, is shown in bottom panel. Scale bars: top panel, 10 μm; bottom panel, 1 μm. **(B)** Time sequence of the cropped region shown in A. See also Video 3. Scale bar = 1 μm. **(C)** Left panel: zoomed in image of the region depicted in black square in bottom panel in A. Right panels: zoomed in images of mobile regions located inside the cell (red arrows in left panel) and an immobile region located outside of the cell (blue arrow in left panel). Scale bars: Left panel, 250nm; Right panels, 100 nm. **(D)** Three-dimensional density analysis of the cell shown in A-C; each row in the Y axis represents a single timepoint, X-axis represents different particle densities and color encodes for the probability of a particle to reside at a given density, in logarithmic scale. Density profiles of additional cells imaged by live-SMLM and a representative single timepoint plot are provided in Figure S8.

Figure 4. **Performing single particle tracking and live-SMLM in the same cell by bioorthogonal labeling** of **EGFR with two Fl-dyes.** COS7 cell transfected with GCE system plasmid and ERGR^{128BCNK} (Figure S1A) and labeled with Tet-AF647 and Cy3 **(A)** A live-SMLM time stack image acquired in the 640 nm channel (Tet-AF647). Color represents single timepoints that were each reconstructed from 150 frames. **(B)** Zoomed in images of four regions depicted in squares in A. **(C)** TIRF image of the same cell captured using 561 nm channel (Cy3). **(D)** Single particle tracks obtained from the zoomed in regions shown in B. Colors represent individual tracks. **(E)** Mean square

displacement plots of particle tracks taken from each of the zoomed in regions shown in B and D. Scale bars: A,C 5 μm; B,D 1 μm.

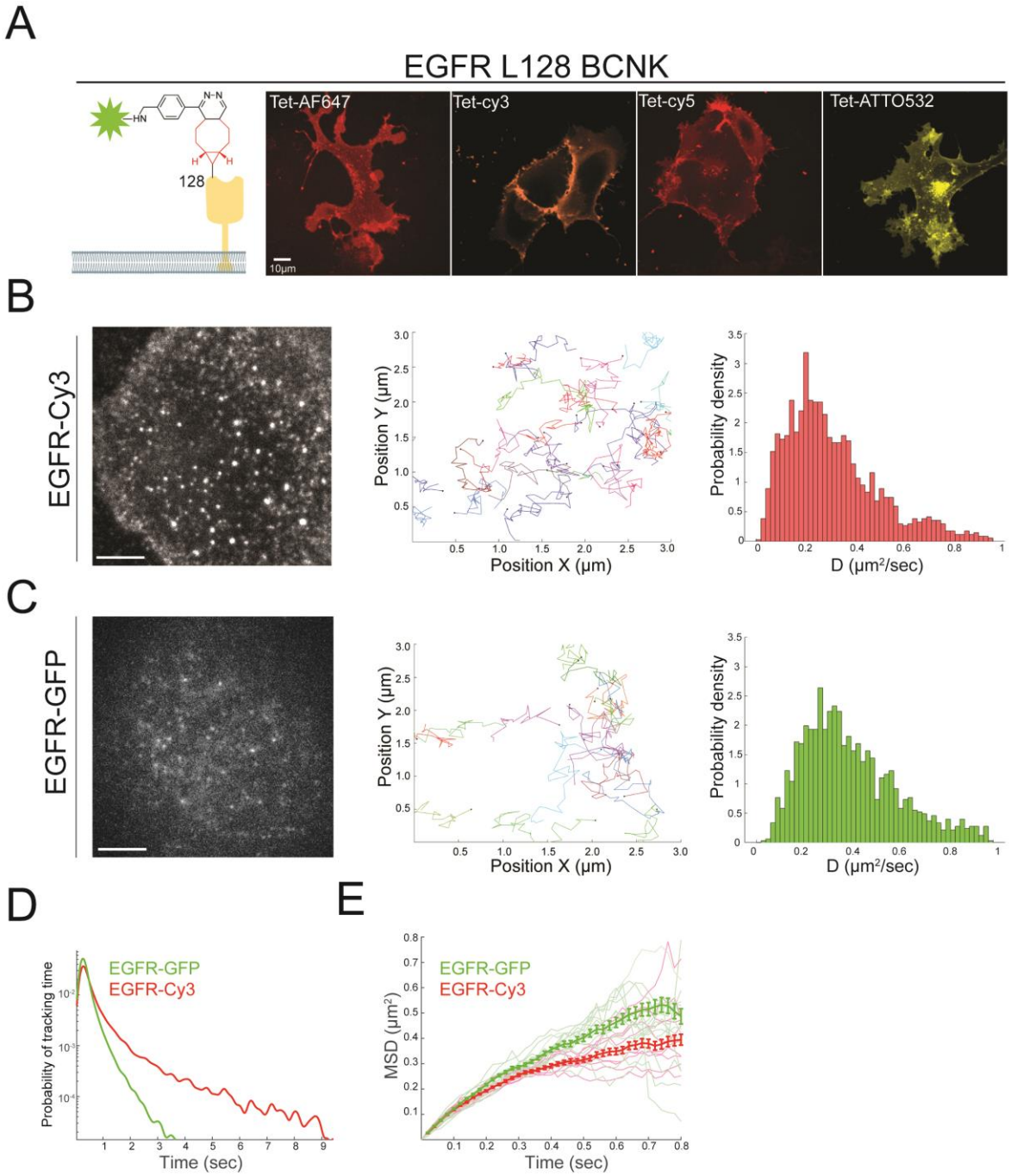
A
EGFR L128 BCNK
128
Tet-AF647
Tet-cy3
Tet-cy5
Tet-ATTO532
10μm
B
EGFR-Cy3
Position Y (μm)
Position X (μm)
Probability density
D (μm²/sec)
C
EGFR-GFP
Position Y (μm)
Position X (μm)
Probability density
D (μm²/sec)
D
EGFR-GFP
EGFR-Cy3
Probability of tracking time
Time (sec)
E
EGFR-GFP
EGFR-Cy3
MSD (μm²)
Time (sec)

Figure 1

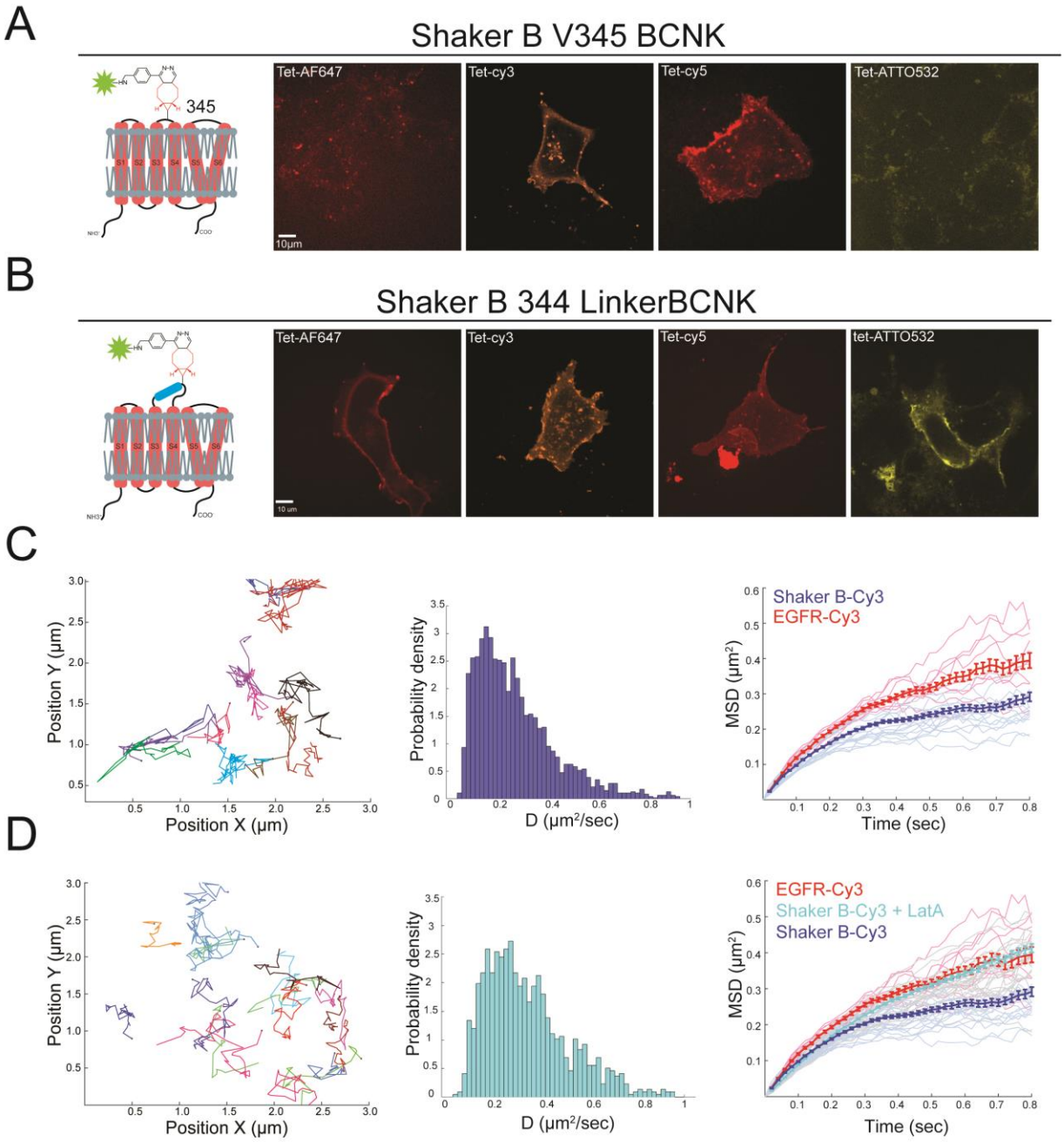
A
Shaker B V345 BCNK
345
Tet-AF647
Tet-cy3
Tet-cy5
Tet-ATTO532
10µm
B
Shaker B 344 LinkerBCNK
Tet-AF647
Tet-cy3
Tet-cy5
tet-ATTO532
C
Position Y (µm)
Position X (µm)
Probability density
D (µm²/sec)
MSD (µm²)
Time (sec)
Shaker B-Cy3
EGFR-Cy3
D
Position Y (µm)
Position X (µm)
Probability density
D (µm²/sec)
MSD (µm²)
Time (sec)
EGFR-Cy3
Shaker B-Cy3 + LatA
Shaker B-Cy3

Figure 2

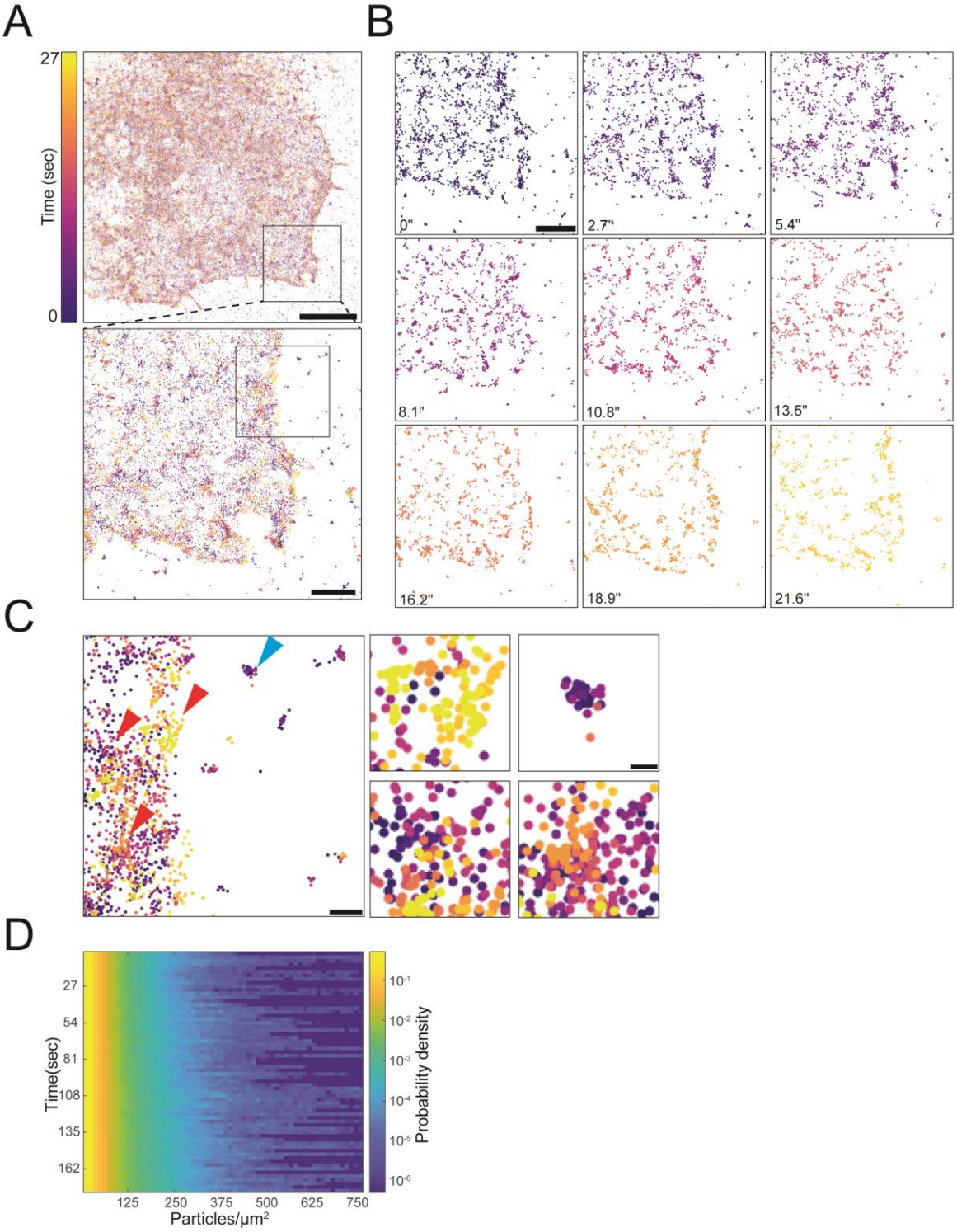
A
B
C
D
27
Time (sec)
0
0"
2.7"
5.4"
8.1"
10.8"
13.5"
16.2"
18.9"
21.6"
Time(sec)
27
54
81
108
135
162
125
250
375
500
625
750
Particles/μm²
Probability density
10⁻¹
10⁻²
10⁻³
10⁻⁴
10⁻⁵
10⁻⁶

Figure 3

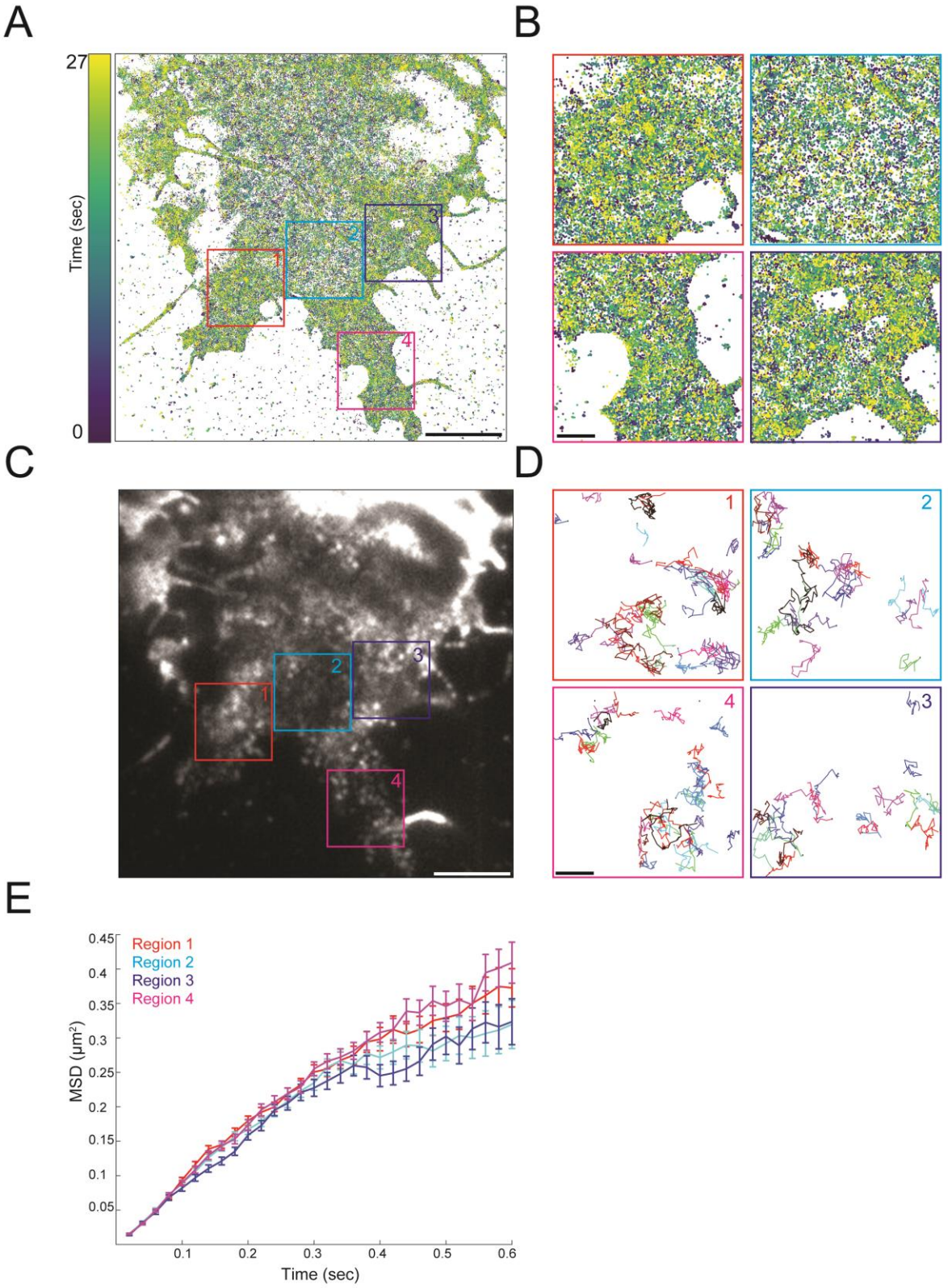
A
B
C
D
E
27
0
Time (sec)
1
2
3
4
Region 1
Region 2
Region 3
Region 4
MSD (μm²)
Time (sec)
0.45
0.4
0.35
0.3
0.25
0.2
0.15
0.1
0.05
0.1
0.2
0.3
0.4
0.5
0.6

Figure 4